Reversing the effects of the Patagonian ice sheet on the southern Andes

Luke Cartwright

Mark Brandon and David Bercovici

May 11, 2016

A Senior Essay presented to the faculty of the Department of Geology and Geophysics, Yale University, in partial fulfillment of the Bachelor's Degree.

Abstract

For a large part of the past 1Ma, the southern andes have been consistently eroding under the weight of the Patagonian ice sheet, which is still present today in the form of the northern and southern Patagonian ice fields. This paper presents a 1-Dimensional Quasi-steady state glacier model, which we have used to determine the change in the topographic profile of the Andes due to glacial erosion. Simulations are then generated along an W-E cross-section of the region, using an Equilibrium Line Altitude based reconstruction of paleoclimate. The specific features of the model will be described, including isostatic flexure, oceanic calving, and ice divide determination. Further, we will demonstrate that glaciers respond quickly enough to small changes in climate that they can be modeled in the steady state over geologic time scales.

1 Context

This paper develops a novel glacial model, which is applied to the Patagonian Andes. By using a Quasi-Steady state approximation to calculate the glacier's profile, we are able to reverse the erosion that has occurred over the past 1Ma.

There are two main approaches to glacial modeling. In the first, glaciologists develop precise and computationally intensive descriptions of ice flow, in order to determine as accurately as possible how the glacier has developed into its present state and will continue to develop. In the second approach, the model is as simplified as possible. By comparing both kinds of models, we are able to develop a better physical understanding of the factors which are actually important to the development of a glacier. The model developed in this paper is one of the latter. The purpose of the model is to determine the general structure of Andes prior to recent glaciation: have the peaks grown sharper or dulled over time?

The primary way in which this model differs from most other glacial models is that it is designed to be run in reverse. Instead of being given a predefined input state and iterating forwards in time, the model is designed to run backwards from the current state. This is simplified greatly by the steady state approximation. Instead of modeling the exact amount of ice at any given time, based on the changing thickness of the ice, we instead assume that the ice reaches a steady state at which the accumulation and melting are balanced.

The region of study for this paper is an W-E cross-section of the Andes, ranging from 76W to 69.5W at a latitude of 46.6S. For all experiments below, we use a one-dimensional grid of 1000 points, which corresponds to a grid spacing of $\Delta x = 496m(3S.F.)$. The majority of the figures in this paper use 5000yr timesteps through 1ma. However, the bifurcation figures use a 100yr timestep over 10000yrs to capture the effect, which occurs only for a short period of time.

2 Steady State

We conducted experiments with the diffusion model described in Oerlemans 2001 and Veen 2013 to prove that using the steady state model is valid. Using the same input criteria as the steady-state model, the diffusion model shows how the ice moves to balance the system before it reaches steady state. The complete system is characterised completely in equations 1 and 2 .

$$D = |\frac{\Delta h_{ice}}{\Delta x}|^{n-1} \times \left(f_d \times T^{n+2} + f_s \times T^n\right) \tag{1}$$

$$H_{t+1,x} = H_{t,x} + \Delta T \times \left(\frac{\Delta}{\Delta x}\left(\frac{\Delta D}{2} \times \frac{\Delta h_{ice}}{\Delta x}\right) + flux_x\right) \tag{2}$$

From figure 1 we can see that the diffusion system reaches a stable equilibrium over the course of about 2ka. This is much smaller than the timescale of the study, and of a similar size to the timesteps used. This means that small changes in the ELA will be quickly reflected by the height of the glacier, and so approximating it with the steady state is perfectly valid.

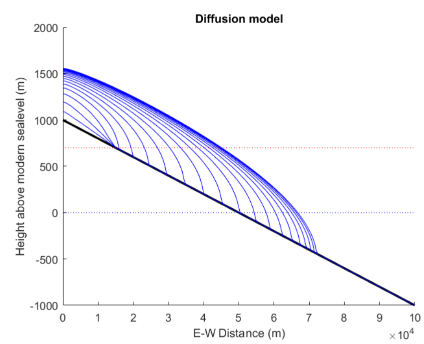

Figure 1: *This graph shows the progression of the diffusion model towards a steady state in 50yr steps up to 1ka.*

3 Computational Model

3.1 General Principle

The computational model is founded on four main principles

1. Glaciers have no slope at their highest point, such that $\frac{\delta h}{\delta x} = 0$.
2. Above some altitude, which we will call the Equilibrium Line Altitude (ELA), snow precipitates onto the glacier. Below this line, snow melts. However, the ELA may not be constant, and the ice flux may vary non-linearly with the height of the surface above or below the ELA.
3. The toe of the glacier follows some common shape.
4. Ice mass is conserved.

From these principles the rest of the model can be derived. In addition to these constraints, there are modifications to the model that allow it to account for flexure, calving and uplift.

The biggest limitation of this method is that it only works on one half of the glacier's profile at a time. In order to form the complete profile of a glacier, the point at which the two profiles split on the landscape has to be found. This point is known as the ice divide, and is where the slope of the glacier goes flat.

All of the calculations in this paper assume a fixed one dimensional spatial grid, such that $\Delta x = x_{i+1} - x_i \forall i$.

3.2 Equilibrium Line Altitude (ELA)

The ice flux is calculated in this model using the equations determined empirically by Hubbard et al. 2005. These calculations are based on the height of the uppermost surface with respect to the ELA.

The biggest variable controlling the ice flux is the ELA, which varies non-linearly along x in the modeled region. In the westernmost marine region, the ELA is determined by a boltzmann sigmoidal function. This is then replaced by a linear increase up to a capped maximum. This is stated concisely in equation 3.

$$ELA_x = \begin{cases} \frac{(a-b)}{(1+\exp^{\frac{(x-c)}{d}})} + b & x \leq x_{ls} \\ ELA_{ls} + (x - x_{ls}) \\ \quad \times (ELA_{max} - ELA_{ls}) & x_{ls} < x \leq x_{le} \\ ELA_{max} & otherwise \end{cases} \tag{3}$$

Using the following table of constants, defined in Hubbard et al. 2005:

a	774	
b	2572	
c	272	
d	64	
ELA_{max}	2800	m
x_{ls}	280	km
x_{le}	330	km

The ELA at a given point of time in the past can be found by shifting the ELA up or down according to the change in temperature given by climate proxies Ma and Brandon 2016.

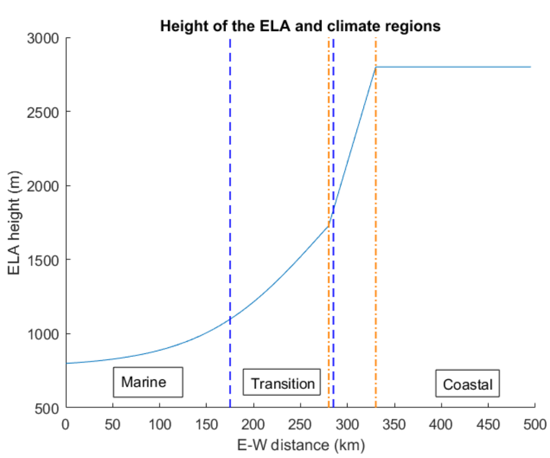

Figure 2: *This graph shows the height of the ELA without any shifting, as well as the various balance rate regions regions. The flux balance rate slowly transitions between the blue dotted lines, while the ELA gradient changes at the orange dotted line from a Boltzmann sigmoidal equation to a linear increase to a flat value.*

3.3 Ice flux

Once the ELA at a given grid point is known, the surface ice flux (B_x) can be found by passing the difference in height between the ELA (ELA_x) and the surface (S_x) through a balance rate function. However, this balance rate function varies across the spatial grid as conditions shift from marine to coastal. A complete description of how this function varies across x is given in equation 4.

$$\lambda_{max} = max\left(0, min\left(1, \frac{(x - x_{marine})}{x_{marine} - x_{coastal}}\right)\right) \times (\lambda_{coastal} - \lambda_{marine}) + \lambda_{marine}$$
$$where \quad \lambda = \{b, z\} \tag{4}$$
$$r = min\left(1, \frac{(S_x - ELA_x)}{z_{max}}\right) \tag{5}$$
$$B = b_{max} \times r(2 - r) \tag{6}$$

Using the following table of constants, defined in Hubbard et al. 2005:

x_{marine}	175	km
$x_{coastal}$	285	km
b_{marine}	4	ma^{-1}
$b_{coastal}$	0.25	ma^{-1}
z_{marine}	1200	m
$z_{coastal}$	425	m

Later on, we will find that we need the integral of the surface flux. We shall call this integral q. To compute this on a well-spaced discrete variable, we define q to be the cumulative trapezoidal integral of the surface flux B, as in equation 7.

$$\int_1^n B\delta x = q_n = (x_n - x_1)\sum_{k=1}^{n}\left[\frac{flux_k + flux_{k+1}}{2}\right] \tag{7}$$

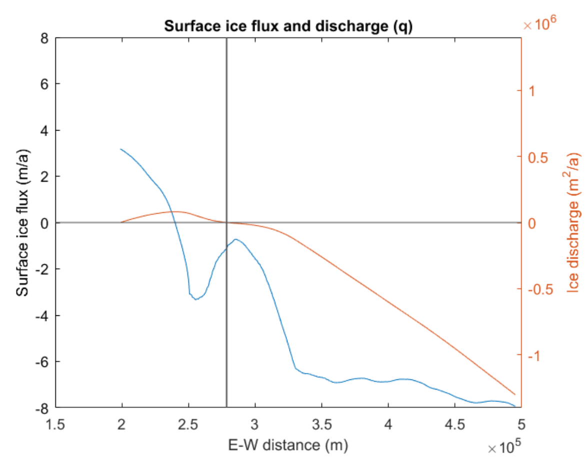

Figure 3: *This graph show the relationship between surface ice flux and its integral, which is also the discharge of the glacier.*

3.4 Toe calculation

At the crossing point x_{nL}, which is the first point at which $q_{nL} <= 0$, all of the accumulated ice has been melted. We therefore know that the toe of the glacier must be located at some point between x_{nL-1} and x_{nL}. We can determine this point more precisely: the terminus occurs at $x_{nL-1} + \delta L$ using linear interpolation as in equation 8.

$$\delta L = -\frac{q_{nL-1}}{\left(\frac{q_{nL} - qnL-1}{\delta x}\right)}; \tag{8}$$

Now that we know the precise position of the toe, we can use it to determine the height of the first grid point upstream from the toe in the glacial profile. For the first grid point, we find the root of the non-linear function described in equation 9. This equation defines the profile of the toe between x_{nL-1} and $x_{nL-1} + \delta L$. Specifically, it states that both the discharge and the ice thickness fall off linearly between these two points, allowing q and T at $x_{nL-1} + \frac{\delta L}{2}$ to be calculated in terms of the q_{nL-1} and T_{nL-1}, leaving a non-linear equation in T_{nL-1}.

$$d - x_c + \frac{\delta x}{T_M} \times \frac{q_M}{T_M^2 * f_d + f_s}^{\frac{1}{n}} \tag{9}$$

$$where \quad q_M = \frac{q(nL-1)}{2}, \quad T_M = \frac{d - h_{nL-1}}{2}$$

3.5 Glacier Profile

The remainder of the profile of the glacier can be calculated upwind of the toe by iterating over all of the points above it. Using the height of the point to the right and the discharge of the glacier, the slope of the glacier is found using equation 10 projected backwards using equation 11.

$$\frac{\delta H}{\delta x} = -\frac{1}{T_{i+1}} \times \frac{q_{i+1}}{T_{i+1}^2 * f_d + f_s}^{\frac{1}{n}} \tag{10}$$

$$H_i = H_{i+1} - \frac{\delta H}{\delta x} \Delta x \tag{11}$$

The glacier profile is constrained on the other side by the fact that there is no slope at the ice divide and therefore $\frac{\delta H}{\delta x}_0 = 0$.

3.6 Isostatic Flexure

The weight of the ice on the crust causes it to depress into the mantle. We can imagine that the bedrock is floating on top of the mantle, and that the system is currently in steady state. If we then make some small change to the weight of the ice, the bed will shift downwards to balance the additional weight against the weight of the displaced mantle. Additionally, we need to consider the case where the height of the bed is below sea level, in which case the displacement of the water has a buoyant effect. All together, this forms equation 12.

$$\Delta H_{bed} = -\frac{\rho_{ice} H_{ice}}{\rho_{mantle}} + \frac{\rho_{water} \times max(-H_{bed}, 0)}{\rho_{mantle}} \tag{12}$$

Local isostacy reduces the height of the bedrock relative to the ELA, which helps to stabilize the system and results in a smaller glacier. The main difficulty here is that we only know the amount that the bed is deflected by after we have calculated the ice profile. This is resolved by iteratively calculating the ice profile and deforming the bedrock. Each iteration the amount of ice will change, but by less and less each time, as the amount that the bed deforms declines with each iteration. This is repeated until the difference between the ice profiles before and after an iteration is a sufficiently small amount.

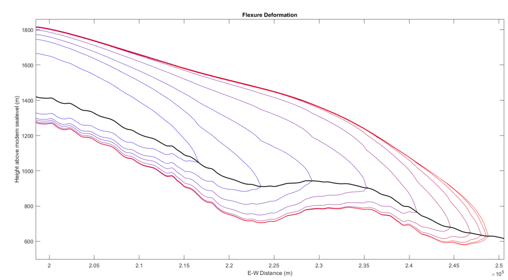

Figure 4: *This deflection of the bed under load from the glacier after each iteration from 1 (red) to 10 (blue)*

3.7 Calving

Ice ceases to have an effect on the rest of the glacier once it reaches the point of floating on the ocean (Oerlemans 2003). This occurs when the weight of the ice is less than the weight of the water that it displaces, as in equation 13.

$$\frac{\rho_{ice} T_{ice}}{\rho_{water} T_{water}} \leq 0 \tag{13}$$

$$where \quad T_{water} = h_{ocean} - h_{bed}$$

We assume that the height of the ocean is 0m for the entire time period of the simulation.

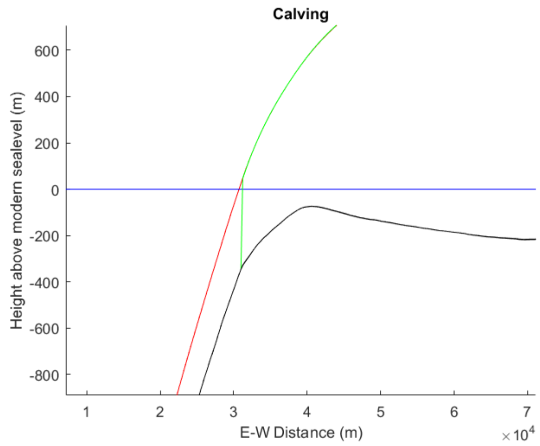

Figure 5: *This graph shows the effect of calving on the glacier. The red line shows the profile of the graph without calving, while the green line shows the profile of the graph with calving.*

3.8 Ice Divide

Since the Ice Divide is located in middle of a large region of surface ice flux, moving the ice divide to the west should enlarge the eastern side of the divide, and shrink the western side. Moving the divide to the east should do the opposite.

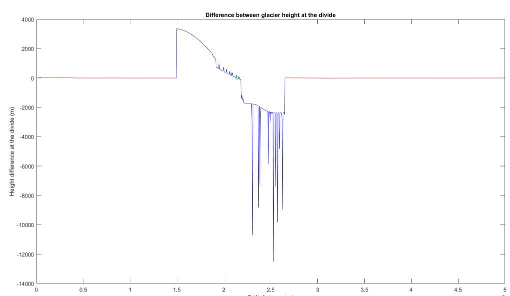

Figure 6: *The difference between the height of the glaciers when the divide is placed at the corresponding point on the x-axis. The regions that result result in no glacier on either side are highlighted in red. The optimal position for the ice divide is circled in green.*

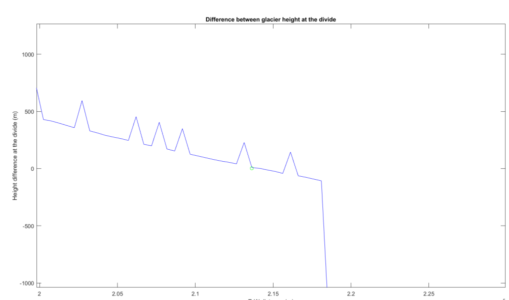

Figure 7: *This is a zoomed in version of 6, showing the non-linear variation in glacial difference across x within a small region.*

If the function were monotonically decreasing, it would be a simple matter to perform a binary search and locate the point at which the divide reaches a minimum. However, due to the small, sharp, inconsistencies that appear when the ice divide is moved, a binary search only helps to narrow the search area.

From the semi-optimal value given by a binary search, we conduct a linear search outwards and in parallel, increasing the range until glacial profile with sufficiently small height disparity is found.

3.9 Erosion

The amount of erosion of the bed is directly related to the sliding velocity u_s by the dimensionless Erosion-Law factor K.

The sliding velocity can be found when calculating the original profile using equation 14

$$u_s = f_s \times T^{n-1} \times |\frac{\delta H_i}{\delta x}|^n \tag{14}$$

which can then be converted directly into an erosion in (m/a) by multiplying it with K.

When the model is running backwards in time the timestep will be negative, depositing material instead of eroding it.

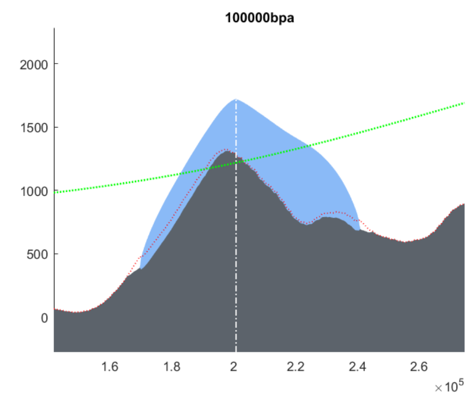

Figure 8: *This figure shows the amount of erosion that occurs over 0.1MA if the ELA is held at the present level. The original bed is shown in red dots, and the gray area shows the level of the bed after 0.1MA.*

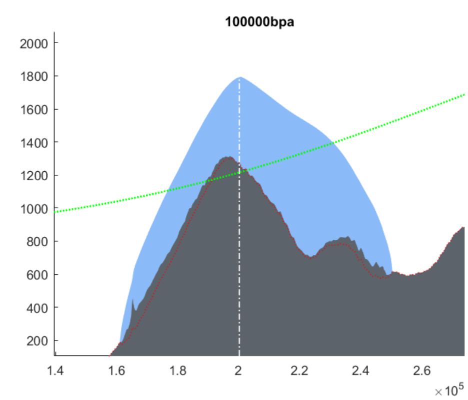

Figure 9: *This figure shows the amount of bedrock required in order to reduce the bed to its present height over 0.1MA if the ELA is held at the present level. The modern bed is shown in red dots, and the gray area shows the original height of the bed.*

3.10 Uplift

Uplift is the counterpart to erosion; it is the reason why the mountains develop despite the constant removal of material. Uplift rates are relatively consistent over the region, and during the modeled time period are very small or non-existent (Gregory-Wodzicki 2000) . Nevertheless, uplift is included in the model for generality, and is simply added to the height of the bed at each time step, as in equation 15.

$$h_{bed} = h_{bed} + uplift \times \Delta T \tag{15}$$

3.11 Bifurcation

Bifurcation refers to the fact that a system can exist in exactly two stable states: one with a large amount of ice (an ice cap), and one with little to no ice (valley glaciers). This is possible because when the ice is low, the surface is lower relative to the ELA, resulting in lower or negative flux values across more of the profile. This results in a much smaller steady state glacier. When the ice is thick, the surface is high relative to the ELA, resulting in higher or positive ice flux across the profile. Both of these situations can result in stable ice configurations: which one the system ends up in is determined by the previous state of the system, since the system requires energy to flip between them. However, when the ELA rises high or low enough, only one of the configurations is possible. This forces the glacier to flip between the two states when the temperature temporarily gets very high or very low.

Herein lies a problem: coming out of the last ice age, we would have expected to follow the original thick-ice configuration shown in blue in figure 10. However, the present day location of the glacier closely corresponds to the low ice configuration shown in orange in the same figure. This figure also shows that the low ice state only became possible within the past 6000-7000 years, and so the transition must have happened some time in this period. Figure 11 shows that both configuration are stable until a ΔELA of around 100-200 is reached, at which point the system would be kicked into the low ice state. The highest that the ΔELA reached was 94m, around 2500bp, which is the most likely point at which this transition would have occurred. The fact that the model does not show this is most likely due to the simplification of physical relationships in the model.

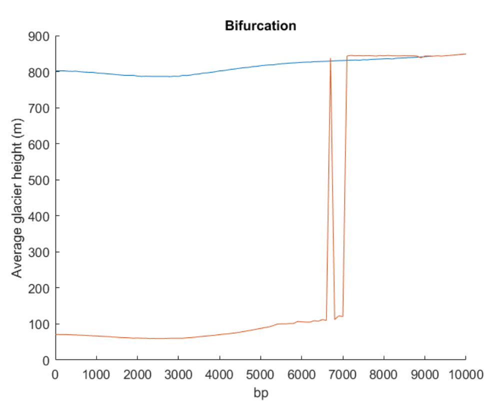

Figure 10: *This shows the two possible high-ice and low-ice bifurcation states over the past 10000 years.*

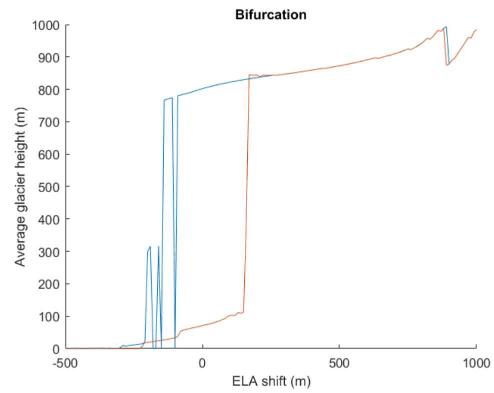

Figure 11: *This shows the two possible high-ice and low-ice bifurcation states at the given ELA shift.*

4 Results

The most problematic result from the model was the exponentially high sliding value at the calving front. There is clearly some behaviour here that is not modeled correctly and needs to be accounted for: most likely the buoyancy from the water is slowing the ice's slide into nothingness. This creates a discontinuity here, which eventually creates a spike in the landscape and causes the model to break down. To fix this, we truncate the sliding values and apply a Gaussian filter. This results in the orange line shown in figure 12.

Over the past 1Ma, Patagonia was mostly underneath deep ice sheets, as shown in figure 13. However, it passes through several interglacial periods like the present. We can see that over 1Ma, very little erosion actually occurs: it clearly takes much longer than this for a glacier to erode down a mountain significantly.

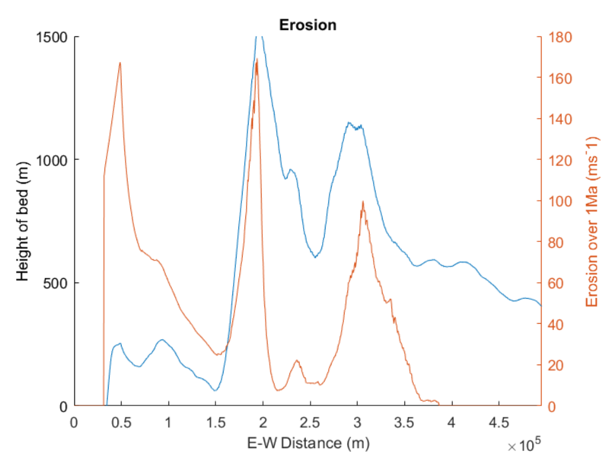

Figure 12: *This figure shows the average rate of erosion across the profile, over 1MA*

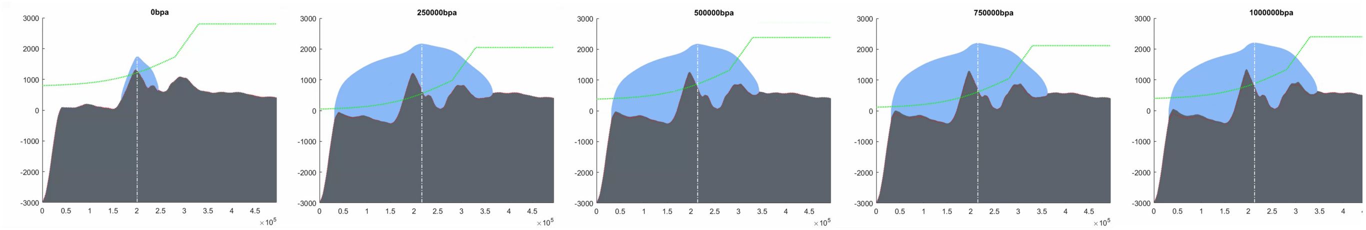

Figure 13: *This figure shows the progression of erosion on the profile over 1MA*

5 Conclusions

1. Glaciers adapt quickly to changes in ELA, meaning that a steady-state approximation is valid.
2. The main action of erosion is to elongate valleys outwards from the ice divide.
3. Erosion over the past 1MA has dulled the smaller, nearby peaks much more than the main peak of mount Valentine.
4. Down-slopes are more quickly eroded than up-slopes.
5. A quasi-steady state model can be run backwards to recover the original landscape with as much accuracy as it can be run forwards to predict the future landscape.
6. The current ELA is within a region that allows for bifurcation, and has been during interglacial periods in the past.

5.1 Limitations

1. ELA is a limited characterization of surface flux, and a complete atmospheric model would be better as we get further into the past.
2. The sliding speed on the calving side of the glacier does not take into account the slow-down effect of the water's buoyancy, resulting in much higher sliding values than are actually observed (by an order of magnitude) as well as a discontinuity at the calving front. This results in much higher rates of erosion than are actually observed.
3. The model doesn't conserve mass, completely ignoring the deposition of moraines.
4. The model becomes unstable if the bed slopes up too quickly, which can happen if there are large discontinuities in the erosion rates.

6 Acknowledgments

I would like to thank Mark Brandon for advising me during this project. His advice and mentorship were essential to the successful completion of this project.

I would also like to thank Keith Ma for providing me with his code to generate a paleoclimate in terms of ELA, and his technical assistance.

Finally, I would like to thank David Bercovici for being the second reader of this paper.

7 References cited

[GW00] Kathryn M Gregory-Wodzicki. "Uplift history of the Central and Northern Andes: a review". In: *Geological Society of America Bulletin* 112.7 (2000), pp. 1091–1105.

[Hub+05] Alun Hubbard et al. "A modelling reconstruction of the last glacial maximum ice sheet and its deglaciation in the vicinity of the Northern Patagonian Icefield, South America". In: *Geografiska Annaler: Series A, Physical Geography* 87.2 (2005), pp. 375–391.

[MB16] Keith Ma and Mark Brandon. "Manuscript". In: (2016).

[Oer01] Johannes Oerlemans. *Glaciers and climate change.* CRC Press, 2001.

[Oer03] J Oerlemans. "A quasi-analytical ice-sheet model for climate studies". In: *Nonlinear processes in geophysics* 10.4/5 (2003), pp. 441–452.

[Vee13] Cornelis J Van der Veen. *Fundamentals of glacier dynamics.* CRC Press, 2013.